CANCER

Immunological mechanisms of the antitumor effects of supplemental oxygenation

Stephen M. Hatfield,[1] Jorgen Kjaergaard,[1] Dmitriy Lukashev,[1] Taylor H. Schreiber,[2]* Bryan Belikoff,[1] Robert Abbott,[1] Shalini Sethumadhavan,[1] Phaethon Philbrook,[1] Kami Ko,[1] Ryan Cannici,[1] Molly Thayer,[1] Scott Rodig,[3] Jeffrey L. Kutok,[3†] Edwin K. Jackson,[4] Barry Karger,[5] Eckhard R. Podack,[2] Akio Ohta,[1] Michail V. Sitkovsky[1,6‡]

Antitumor T cells either avoid or are inhibited in hypoxic and extracellular adenosine-rich tumor microenvironments (TMEs) by A2A adenosine receptors. This may limit further advances in cancer immunotherapy. There is a need for readily available and safe treatments that weaken the hypoxia–A2-adenosinergic immunosuppression in the TME. Recently, we reported that respiratory hyperoxia decreases intratumoral hypoxia and concentrations of extracellular adenosine. We show that it also reverses the hypoxia-adenosinergic immunosuppression in the TME. This, in turn, stimulates (i) enhanced intratumoral infiltration and reduced inhibition of endogenously developed or adoptively transfered tumor-reactive CD8 T cells, (ii) increased proinflammatory cytokines and decreased immunosuppressive molecules, such as transforming growth factor–β (TGF-β), (iii) weakened immunosuppression by regulatory T cells, and (iv) improved lung tumor regression and long-term survival in mice. Respiratory hyperoxia also promoted the regression of spontaneous metastasis from orthotopically grown breast tumors. These effects are entirely T cell– and natural killer cell–dependent, thereby justifying the testing of supplemental oxygen as an immunological coadjuvant to combine with existing immunotherapies for cancer.

INTRODUCTION

T lymphocytes and natural killer (NK) cells are inhibited in hypoxic and extracellular adenosine-rich, inflamed (*1*), and cancerous tissues (*2*, *3*) because of immunosuppressive adenosine 3′,5′-monophosphate (cAMP)–mediated signaling, triggered by A2A adenosine receptors (A2ARs). A2ARs interfere with the trafficking and activities of T and NK cells because of the heterologous desensitization of chemokine receptors and reduced proinflammatory cytokines (*2*, *4*). Hypoxia-A2AR–mediated signaling may also recruit and/or further amplify other immunosuppressive mechanisms (*5*, *6*) in the tumor microenvironment (TME), thereby limiting further advances in promising immunotherapies of cancer (*7*–*13*). This may explain the paradoxical coexistence of tumors and antitumor T cells in cancer patients and mice (*6*, *14*). This view is supported by findings of enhanced T cell– and NK cell–mediated tumor rejection in mice that are genetically deficient in A2AR (*2*,*15*) or adenosine-generating CD39/CD73 (*13*, *16*–*19*) or in the presence of A2AR antagonists (*2*, *19*, *20*). In addition, the overexpression of extracellular adenosine-generating CD73 on human breast tumors and A2 adenosine receptors on antitumor immune cells was implicated in the protection of tumors from chemotherapy and immunotherapy (*21*).

Thus, there is strong justification and motivation to develop safe treatments that weaken the hypoxia-driven and CD39/CD73-mediated accumulation of extracellular adenosine and immunosuppressive signaling through A2AR on T and NK cells in the TME by targeting CD39 or CD73 ectoenzymes (*13*, *16*–*19*) or by antagonizing the A2AR (*2*, *3*, *6*, *13*). We hypothesized that the reduction of tumor hypoxia using clinical supplemental oxygen protocols (*22*–*24*) may inhibit the hypoxia-driven accumulation of extracellular adenosine in the TME (*25*) and weaken the A2AR-mediated immunosuppression. This, in turn, may further improve cancer immunotherapy approaches and enable tumor regression by unleashing antitumor T and NK cells.

To test this hypothesis, tumor-bearing mice were placed in chambers with well-controlled gas composition (60% oxygen) to mimic protocols of supplemental oxygen delivery to humans (*22*–*24*). This immunological mechanism-based motivation to use respiratory hyperoxia (60% oxygen) as an anti-adenosinergic treatment is conceptually different from the classic approach to generate reactive oxygen species (ROS) in radiotherapy and photodynamic therapy of cancer by breathing 95% O_2/5% CO_2 (carbogen) (*26*–*29*).

RESULTS

Respiratory hyperoxia has antitumor effects

In studies of the weakly immunogenic MCA205 fibrosarcoma pulmonary tumor model with a predictable time course and intensity of T cell response (*30*, *31*), mice breathing 60% oxygen demonstrated improved regression of lung tumors (Fig. 1A). Tumor regression was observed in mice with established lung tumors (11 days) treated with respiratory hyperoxia, long after tumor inoculation (day 11, identified in Fig. 1A as "60% O_2*"). An even stronger regression was observed when mice were treated with respiratory hyperoxia starting immediately after tumor inoculation until assay completion on day 21 (identified as "60%

[1]New England Inflammation and Tissue Protection Institute, Northeastern University, 360 Huntington Avenue, Boston, MA 02115, USA. [2]Department of Microbiology and Immunology, University of Miami Miller School of Medicine, Miami, FL 33136, USA. [3]Department of Pathology, Brigham and Women's Hospital, Harvard Medical School, 20 Shattuck Street, Boston, MA 02115, USA. [4]Department of Pharmacology and Chemical Biology, University of Pittsburgh School of Medicine, Pittsburgh, PA 15219, USA. [5]Barnett Institute of Chemical and Biological Analysis, Northeastern University, Boston, MA 02115, USA. [6]Cancer Vaccine Center, Dana-Farber Cancer Institute, Harvard Institutes of Medicine, 44 Binney Street, Boston, MA 02115, USA.
*Present address: Heat Biologics Inc., 801 Capitola Drive, Durham, NC 27713, USA.
†Present address: Infinity Pharmaceuticals Inc., 780 Memorial Drive, Cambridge, MA 02139, USA.
‡Corresponding author. E-mail: m.sitkovsky@neu.edu

O_2"). Hyperoxia-induced tumor regression was also observed in the poorly immunogenic B16 melanoma pulmonary tumor model (Fig. 1B). Using a less aggressive model of induced metastasis, respiratory hyperoxia (60% O_2) commencing after tumor inoculation resulted in the complete regression of lung tumors and survival of 40% of mice compared to mice breathing ambient 21% O_2 (Fig. 1C). The data in Fig. 1D also demonstrate reduced lung tumor nodules in the spontaneously metastasizing 4T1 triple-negative breast cancer (TNBC) model when mice with 7-day established orthotopic tumors were treated with respiratory hyperoxia. The 4T1 tumor cells express high levels of the adenosine-generating ectoenzyme CD73 to mimic drug-resistant TNBC (*21*).

These data provide support for the clinical testing of anti–A2-adenosinergic interventions, including systemic oxygenation (*25*), as treatments for chemotherapy-resistant TNBC. Indeed, the overexpression of CD73 by TNBC and subsequent adenosine-A2AR/A2BR–mediated immunosuppression in the TME was shown to contribute to resistance to chemotherapy in the analysis of more than 6000 triple-negative and chemotherapy-resistant breast cancers (*21*).

The antitumor effects of respiratory hyperoxia require the activities of endogenous T and NK cells

We tested whether the observed antitumor effects of respiratory hyperoxia were mediated by the increased activities of endogenously developed tumor-reactive T and NK cells or, alternatively, represent the result of direct cytotoxicity or oxidative stress–mediated tumor damage caused by ROS generated by hyperoxia (*26*–*29*) or formed independently of hyperoxia during purine metabolism.

To discriminate between these mechanisms, we tested whether the hyperoxia-induced tumor regression would still be observed in mice genetically deficient in T and NK cells (*24*) [common gamma (γc)/*Rag-2*$^{-/-}$ mice] or in tumor-bearing wild-type mice treated with ROS scavengers. It was expected that if the antitumor effects were the result of ROS generated by 60% oxygen, then respiratory hyperoxia would be capable of inducing tumor regression even in the absence of T and/or NK cells.

Figure 2A and fig. S1 demonstrate that the improved tumor regression seen in wild-type mice breathing 60% oxygen was lost in γc/*Rag-2*$^{-/-}$ mice breathing 60% oxygen. This established the necessity of tumor-reactive T and NK cells for the hyperoxia-enhanced antitumor response. These data also serve as genetic controls indicating that hyperoxia has no effect on tumor seeding or colonization, because breathing 60% oxygen immediately after tumor inoculation did not reduce the number or size of lung tumors in γc/*Rag-2*$^{-/-}$ mice. Similarly, the tumor-regressing effects of hyperoxia were observed in wild-type mice with established tumors even when hyperoxic exposure began after the 11th day of tumor growth, after seeding and colonization (Fig. 1A). Independent confirmation of the lack of effects of 60% oxygen–generated ROS was provided by testing the effects of a ROS scavenger [*N*-acetylcysteine (NAC)] on lung tumor growth in mice treated with respiratory hyperoxia (*26*–*29*). Figure S2

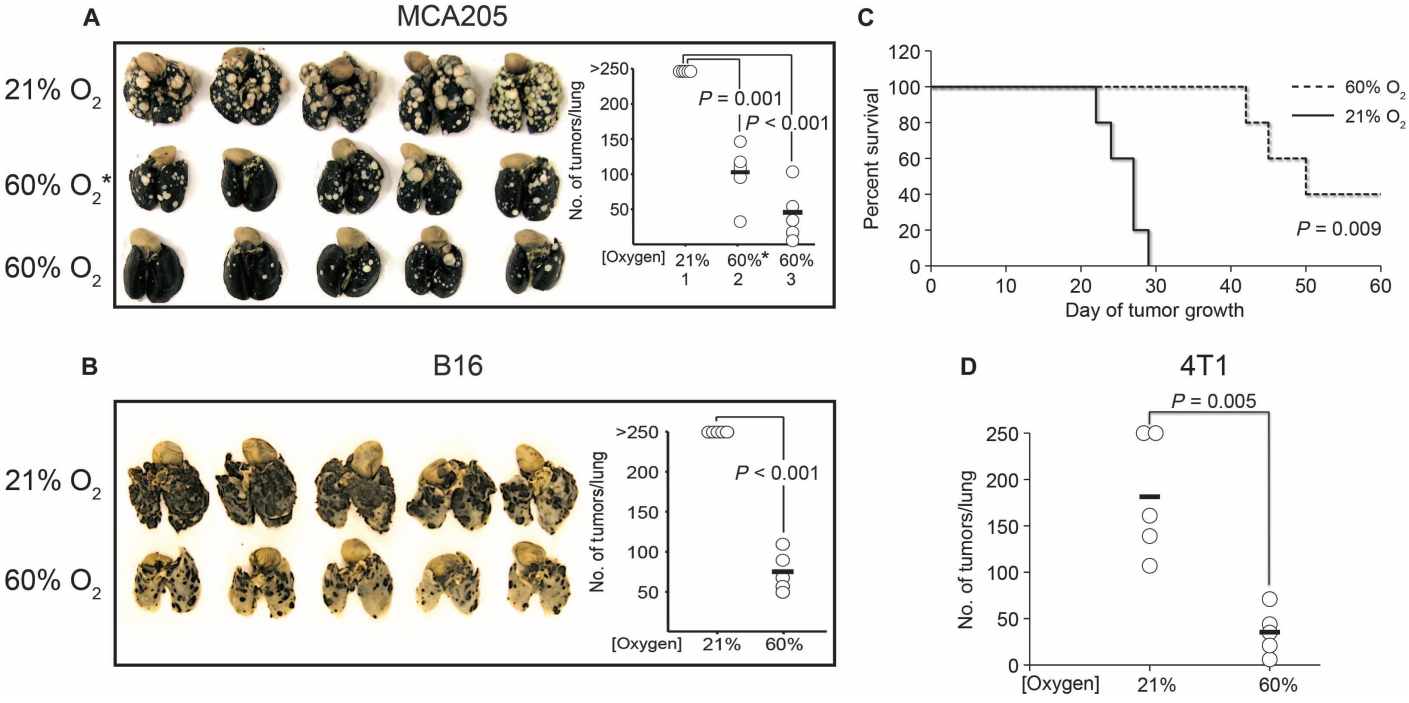

Fig. 1. Respiratory hyperoxia promotes tumor regression and survival and decreases metastasis. (**A**) Respiratory hyperoxia promotes tumor regression in mice with 11-day established MCA205 pulmonary tumors. Mice were placed in chambers with 60% oxygen after 11 days of tumor growth (identified as 60% O_2*; $P = 0.001$), and lungs were harvested at day 21. Stronger regression was observed when mice were placed in 60% oxygen units immediately after tumor inoculation (identified as 60% O_2; $P = 0.0003$) ($n = 5$ mice per group, averages represented as horizontal bars). (**B**) Hyperoxia-enhanced tumor regression in mice with B16 melanoma pulmonary tumors ($n = 5$ mice per group, averages represented as horizontal bars; $P = 0.0001$). (**C**) Respiratory hyperoxia leads to long-term survival in 40% of MCA205 tumor–bearing mice ($n = 5$ mice per group; $P = 0.009$). (**D**) Respiratory hyperoxia strongly decreases spontaneous lung metastasis of orthotopically grown 4T1 breast tumors ($n = 5$ mice per group; $P = 0.005$). Balb/c mice were injected in the third mammary fat pad with 4T1 tumor cells. After tumors became palpable at day 7, mice were placed in either 21 or 60% oxygen until assay completion on day 28.

demonstrates that daily treatment with NAC at doses that are shown to reduce ROS in positive control assays (fig. S2A) does not significantly inhibit the tumor-regressing effects of respiratory hyperoxia (fig. S2B).

To determine the relative contribution of different immune cell subsets in the hyperoxia-induced tumor regression, wild-type mice were depleted of T and NK cells using monoclonal antibodies (mAbs). Figure 2B shows that the improved regression of pulmonary tumors by 60% oxygen is mediated to a large extent by endogenous T cells, because mice depleted of CD4 and CD8 cells demonstrated severely impaired tumor regression after respiratory hyperoxia.

The depletion of NK cells alone virtually eliminated the antitumor effects of respiratory hyperoxia, although NK cell–depleted mice still retained CD4 and CD8 T cells. Although it has been well established that NK cells are important in antitumor immunity (*32*, *33*), our data suggest that the full antitumor potential of NK cells may not be realized because of hypoxia–A2-adenosinergic inhibition in the TME. These in vivo observations also extend previous in vitro demonstrations (*4*) of the high susceptibility of NK cells to A2AR-mediated inhibition. This is further supported by the data in fig. S3, demonstrating hypoxia and A2AR-mediated inhibition of NKG2D expression, NK cell activation, and cytokine secretion.

Thus, respiratory hyperoxia may enhance the antitumor activities not only of T cells but also of NK cells. These data extend previous observations of the critical importance of NK cells in enabling T cell–mediated tumor regression under normal oxygen conditions (*32*, *33*).

Respiratory hyperoxia acts upstream of the hypoxia-adenosinergic pathway

Because we recently established that breathing 60% oxygen was capable of reducing hypoxia and adenosine in the TME (*25*), we hypothesized that respiratory hyperoxia might block the upstream stage of the hypoxia-adenosine-A2AR–mediated immunosuppressive pathway in the TME (*6*). If so, then hyperoxia would not be able to further improve tumor regression in A2AR$^{-/-}$ mice as compared to wild-type mice (*2*). In agreement with this hypothesis, Fig. 2C (right side) demonstrates that respiratory hyperoxia did not further improve tumor regression in A2AR$^{-/-}$, suggesting that the reversal of hypoxia was acting upstream of A2AR signaling. This conclusion was confirmed in adoptive transfer experiments, where respiratory hyperoxia enhanced the therapeutic efficacy of wild-type T cells, but not A2AR$^{-/-}$ T cells (fig. S4). Data from Fig. 2C (identified as "21% WT" versus "21% A2AR$^{-/-}$") also extend previous observations of the enhanced rejection of intradermal tumors in A2AR$^{-/-}$ mice (*2*) to the pulmonary foci tumor model. Together, data in Figs. 1 and 2 provide genetic evidence that hyperoxia prevents the inhibition of antitumor T and NK cells by acting upstream of the hypoxia-[adenosine]^{High}-A2AR-[cAMP]^{High} pathway.

In support of the hypothesis that the reversal of hypoxia in the TME prevents the inhibition of antitumor immunity, analysis of tumors in different anatomical locations shows markedly fewer CD8 and CD4 T cells in hypoxic areas of tumors compared to normoxic neighboring regions of the same tumor (Fig. 3A and fig. S5). This demonstration that T cells seem to avoid hypoxia provides an explanation of the limited tumor infiltration by T cells and the less than optimal clinical outcomes of the immunotherapies in cancer (*34*).

Using a molecular in vivo hypoxia marker (*25*), Fig. 3 (B and C) demonstrate that respiratory hyperoxia reduced the exposure of lymphocytes to hypoxia in the TME as well as in lymphoid organs. Both CD8 and CD4 T cells from the lungs and spleen of tumor-bearing mice breathing 60% oxygen had less hypoxic staining. These observations extend and support our previous data demonstrating that respiratory hyperoxia decreased intratumoral hypoxia and the concentrations of extracellular adenosine in the TME (*25*).

Respiratory hyperoxia converts an immunosuppressive TME into an immunopermissive TME

Additional analysis of the TME demonstrated that the conversion to an immunopermissive TME by respiratory hyperoxia resulted in the highly desirable (*34*) enhancement of tumor infiltration by antitumor CD8 T cells (Fig. 4A). This was confirmed and extended in a flow cytometric time course assay showing the hyperoxia-enhanced accumulation of highly activated CD8 T cells in the pulmonary TME (Fig. 4B). Mice with established pulmonary tumors treated with respiratory hyperoxia demonstrated an increase in the number of CD8$^+$, CD69$^+$, and CD44$^+$ cells in the TME. Because T cells demonstrate aversion to hypoxia (Fig. 3A), the reduction in the exposure of T cells to hypoxia in the TME after hyperoxic breathing may explain their increased presence

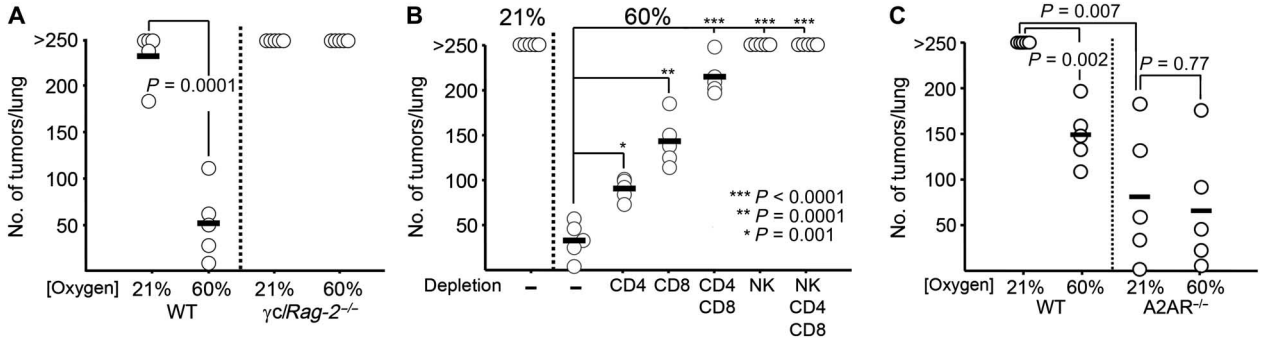

Fig. 2. Antitumor effects of respiratory hyperoxia require endogenous T and NK cells. (**A**) Tumor-regressing effects of hyperoxia are lost in γc/*Rag-2*$^{-/-}$ mice deficient in T and NK cells. MCA205 tumor–bearing wild-type (WT) or γc/*Rag-2*$^{-/-}$ mice were placed in 21 or 60% oxygen after tumor inoculation, and lung tumors were assessed after 21 days ($n = 5$ mice per group, averages represented as horizontal bars; $P = 0.0001$). (**B**) Hyperoxia-induced regression of MCA205 pulmonary tumors is mediated by CD4, CD8, and NK cells. Depletion of different T cell subsets or NK cells using mAbs 2 days before tumor inoculation impaired or completely abrogated the antitumor effects of 60% oxygen ($n = 5$ mice per group, averages represented as horizontal bars; *$P = 0.001$, **$P = 0.0001$, ***$P < 0.0001$). (**C**) Respiratory hyperoxia improves tumor regression in MCA205 tumor–bearing WT mice but does not significantly improve the therapeutic benefit of genetic elimination of A2AR ($n = 5$ mice per group, averages represented as horizontal bars; $P = 0.002$ and $P = 0.77$ for WT and A2AR$^{-/-}$, respectively).

in the TME. In these assays, the recruitment of CD4 T cells was not affected, suggesting that respiratory hyperoxia may differentially affect CD8 versus CD4 T cells. This could be due to changes in the cytokine/chemokine profile in the TME after respiratory hyperoxia or differences in the expression of chemokine receptors.

In Fig. 4 (C and D), we used custom-made reverse transcription polymerase chain reaction (RT-PCR) arrays to scan the pulmonary TME for hyperoxia-induced changes among 94 proinflammatory and tolerogenic mediators, including 4 chemokine receptors, 20 chemokine ligands, and 27 different cytokines and chemokines (*35*). The hyperoxia-associated increase in the levels of proinflammatory cytokines [IL-2 (interleukin-2) and IL-12] and chemokines [CXCL9 (CXC motif ligand 9), CXCL10, and CXCL11] (Fig. 4C) was accompanied by the simultaneous decrease in the immunosuppressive cytokine transforming growth factor–β (TGF-β) (Fig. 4D).

Respiratory hyperoxia may weaken immunosuppression by regulatory T cells in the TME

Experiments in Fig. 5A addressed a well-appreciated problem in clinical immunotherapy protocols, which is the presence of suppressive regulatory T cells (T_{regs}) in the TME that inhibit the antitumor immune response (*36*). We hypothesized that respiratory hyperoxia may decrease immunosuppression by T_{regs} in the TME because of the proposed role of hypoxia and cAMP response element (HRE/CRE)–mediated transcription in the development and function of T_{regs} (*5*). To this end, we analyzed the effect of respiratory hyperoxia on the time course of $CD4^+$, $CD25^+$, $Foxp3^+$ T_{reg} tumor infiltration and the expression of negative regulators of the immune response.

Data from Fig. 5 suggest that hyperoxia weakens T_{reg}-mediated suppression of the immune response in the pulmonary TME by four distinct mechanisms. Respiratory hyperoxia resulted in (i) a decrease in the percentage of T_{regs} in the pulmonary TME (Fig. 5A, left), (ii) reduced levels of the transcription factor Foxp3 in T_{regs} (Fig. 5A, right), (iii) reduced expression of the adenosine-generating enzymes CD39/CD73 on T_{regs} (Fig. 5, B and C), and (iv) a decrease in the expression of CTLA-4 (cytotoxic T lymphocyte–associated protein 4) on T_{regs} (Fig. 6A), which has been shown to be critical for T_{reg}-mediated suppression (*37*).

In accordance with data from Fig. 3 on CD4 and CD8 T cells in the TME, T_{regs} from tumor-bearing mice breathing 60% oxygen demonstrated less exposure to hypoxia (Fig. 6B). Because respiratory hyperoxia reduced CTLA-4 on T_{regs} (Fig. 6A) and CTLA-4 is important for the functions of T_{regs} (*37*), the relationship between hypoxia and CTLA-4 expression on T_{regs} was further evaluated. Figure 6C and fig. S6 demonstrate that CTLA-4^{High} T_{regs} from the lung TME and spleen of tumor-bearing mice were exposed to lower oxygen tension when compared to CTLA-4^{Low} T_{regs}. Although both CTLA-4^{High} and CTLA-4^{Low} T_{regs} were present in mice breathing 21% and 60% oxygen, the hypoxia staining from the CTLA-4^{High} T_{reg} population was lower in hyperoxia-treated mice. This,

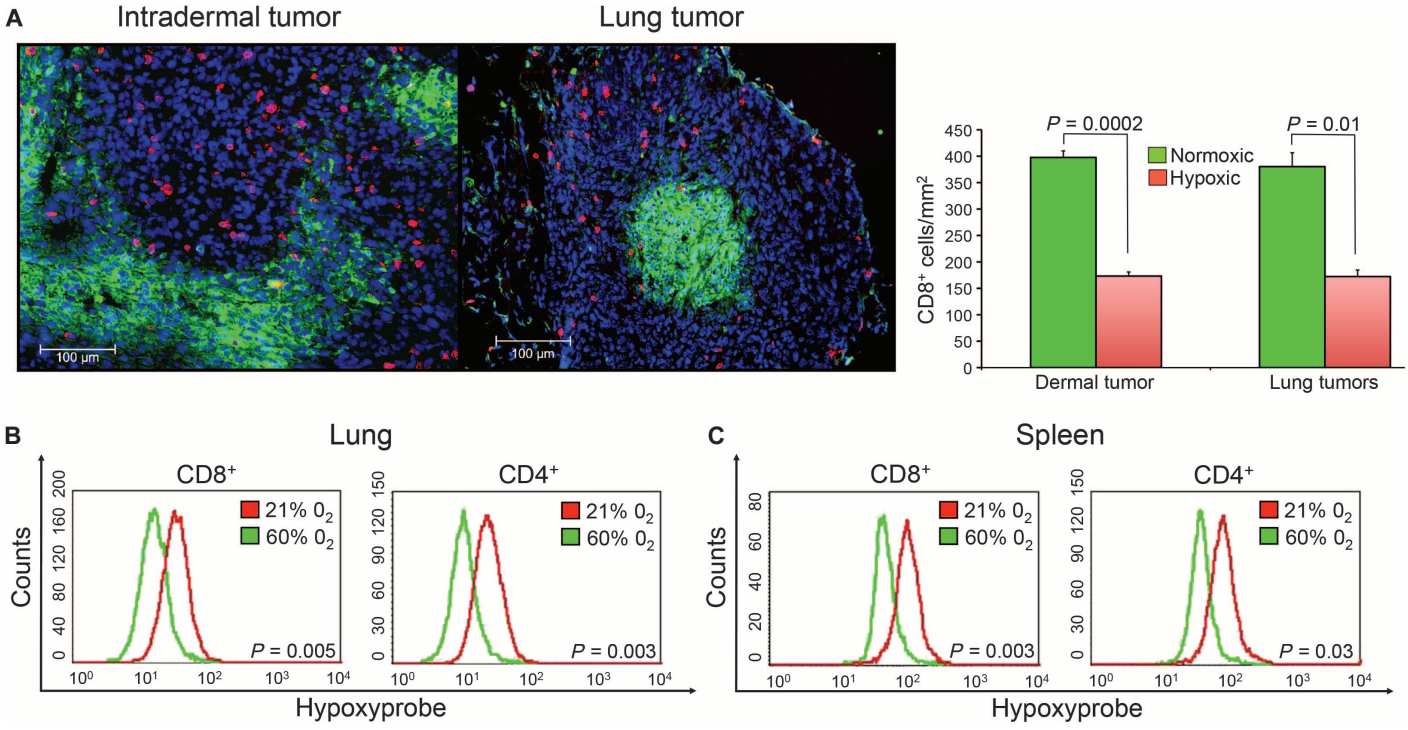

Fig. 3. Antitumor T cells avoid hypoxic areas of the TME. (**A**) Immunohistochemical demonstration of CD8 T cells (red) preferentially localized outside of hypoxic areas (green) of intradermal (left panel) and lung (right panel) TME. Tissue sections from 14-day established lung or intradermal MCA205 tumors were analyzed. Statistical comparison between hypoxic and normoxic locations of CD8 T cells seen in the representative images on the left (scale bar, 100 μm) is shown in the histogram on the right (dermal: $n = 3$ mice, $P = 0.0002$; lung: $n = 3$ mice, $P = 0.01$). (**B**) Respiratory hyperoxia decreases hypoxic exposure of CD4 and CD8 T cells in the lung TME and spleen of tumor-bearing mice. Lymphocytes were isolated from MCA205 tumor–bearing lungs or spleen of mice breathing 21 or 60% oxygen, and the mean fluorescence intensity (MFI) of Hypoxyprobe-labeled T cells was analyzed by flow cytometry (lung: $n = 4$ mice per group; CD8 $P = 0.005$, CD4 $P = 0.003$; spleen: $n = 3$ mice per group; CD8 $P = 0.003$, CD4 $P = 0.03$).

in turn, may inhibit HRE- and CRE-mediated immunosuppressive transcription of suppressive mediators, such as TGF-β (Fig. 4D) (*5*).

To extend the studies of endogenously developed tumor-reactive T cells and to gain additional mechanistic insights into hyperoxia-mediated enhancement of tumor regression, we studied adoptively transferred tumor-reactive T cells in mice breathing 60% oxygen. Mice with 11-day established pulmonary tumors were infused intravenously with in vitro culture-activated antigen-specific T cells (fig. S7) derived from tumor-draining lymph nodes (TDLNs). Twenty-four hours before transfer, mice were treated with cyclophosphamide to mimic clinical protocols of adoptive cell transfer (*30*, *31*). As shown in Fig. 7A, commencing respiratory hyperoxia on the same day as adoptive T cell immunotherapy in mice with 11-day established tumors enhanced tumor regression when compared to mice treated with T cells alone (Fig. 7A; 60%*). An even stronger therapeutic effect, shown by the complete regression of lung tumors by adoptively transferred tumor-reactive T cells, was achieved if mice were breathing 60% oxygen from the time of tumor inoculation until the assay completion on day 21 (Fig. 7A; 60%). In control assays, adoptively transferred tumor-reactive $A2AR^{-/-}$ T cells demonstrated no improved efficacy when combined with respiratory hyperoxia (fig. S4).

Because limited tumor infiltration of antitumor T cells has been shown to diminish the effects of immunotherapy, we examined the trafficking of adoptively transferred tumor-reactive T cells in the TME. Figure 7B shows the facilitation of intratumoral infiltration and the increased number of carboxyfluorescein diacetate succinimidyl ester (CFSE)–labeled adoptively transferred T cells in pulmonary tumors of mice treated with respiratory hyperoxia. These results are complementary to and extend the observation of increased intratumoral infiltration of endogenously developed CD8 T cells in mice breathing 60% oxygen (Fig. 4, A and B). Respiratory hyperoxia also increased the production of interferon-γ (IFN-γ) by adoptively transferred ($Thy1.1^+$) and endogenously developed ($Thy1.2^+$) tumor-reactive T cells from the pulmonary TME (fig. S8).

Because data from Fig. 2 (A and B) pointed to the importance of NK cells in the hyperoxia-induced tumor regression, we also examined the effect of respiratory hyperoxia on adoptively transferred activated NK cells. Figure S3D demonstrates that respiratory hyperoxia enhanced the tumoricidal activities of transferred NK cells against established B16 pulmonary tumors. Confirming and extending data from Fig. 1B, respiratory hyperoxia improved tumor regression of established B16 tumors even in the absence of NK cell transfer. However, combination with adoptive transfer of NK cells resulted in the strongest tumor regression. The hyperoxia-mediated enhancement of NK cell activity occurred without adjunctive IL-2 therapy, which is often critical for effective NK cell therapy (*38*).

Additional studies also determined whether the antitumor effects of supplemental oxygen could be accomplished by less than 60% oxygen. Figure 7C demonstrates in dose-response studies that breathing as low as 40% oxygen was also capable of promoting tumor regression. By alternating the breathing of 60% oxygen with 40 or 21% oxygen every 12 hours, we established that breathing 60% oxygen 24 hours/day was

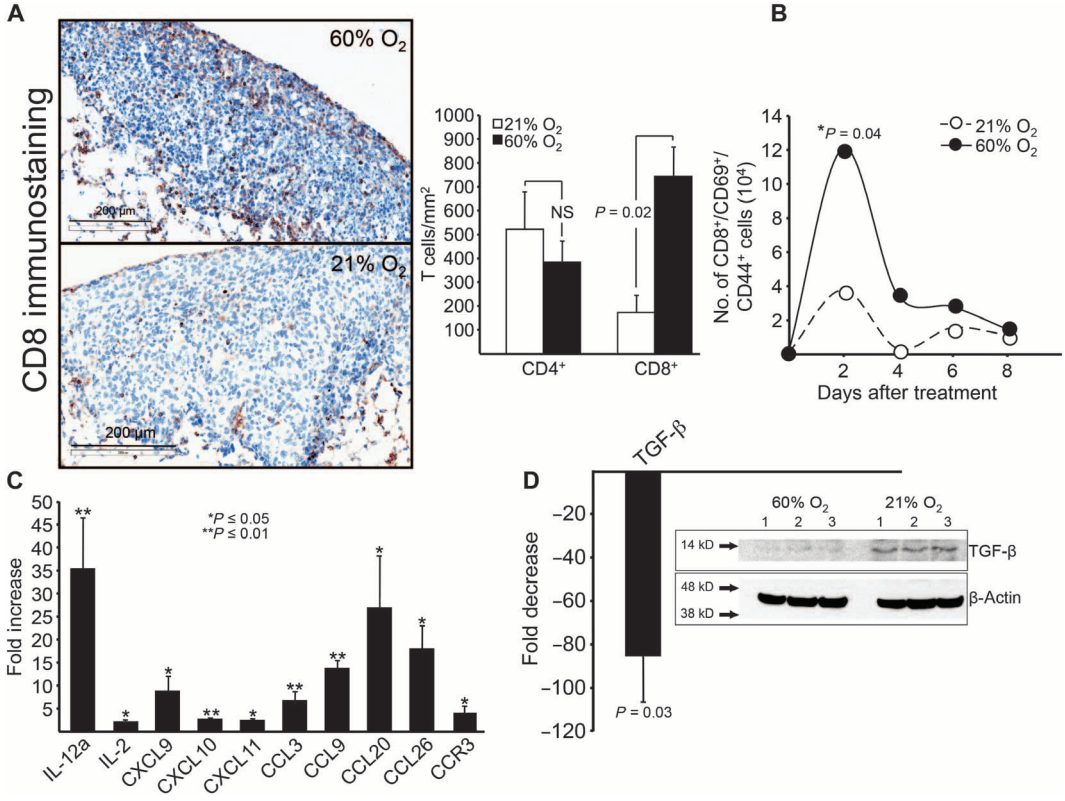

Fig. 4. Respiratory hyperoxia results in an immunopermissive TME. (**A**) Immunohistochemical demonstration of the enhanced infiltration of endogenous CD8 T cells into established MCA205 pulmonary tumors due to hyperoxic breathing (means ± SEM, $P = 0.015$; $n = 3$ mice per group; scale bar, 200 μm). (**B**) Hyperoxic breathing promotes the accumulation of highly activated endogenous CD8 T cells as shown by flow cytometric analysis of the pulmonary TME. Mice with 11-day established MCA205 pulmonary tumors were treated with respiratory hyperoxia for 4 days, and the number of $CD8^+$, $CD69^+$, and $CD44^+$ cells was analyzed by flow cytometry (means ± SEM, $*P = 0.04$; $n = 3$ mice per group). (**C**) Respiratory hyperoxia increases the levels of immunostimulating cytokines and chemokines as detected using custom-made RT-PCR arrays to screen for changes in 94 different chemokines and cytokines. Mice with 11-day established MCA205 pulmonary tumors were treated with respiratory hyperoxia for 72 hours (means ± SEM, exact *P* values listed in table S1; $n = 3$ mice per group). (**D**) Respiratory hyperoxia decreases the levels of TGF-β in the lung TME (means ± SEM, $P = 0.03$; $n = 3$ mice per group). Inset: Immunoblot for TGF-β in lung tumors from mice breathing 21 and 60% oxygen. Mice with 11-day established MCA205 pulmonary tumors were treated with respiratory hyperoxia for 72 hours.

necessary to achieve the strongest antitumor effects (Fig. 7D). Because CTLA-4/PD-1 (programmed cell death protein 1) blockade represents one of the most important recent advances in cancer immunotherapy (*8*–*12*), we also tested whether respiratory hyperoxia would be capable of enhancing the therapeutic efficacy of CTLA-4/PD-1 blockade against pulmonary tumors. Figure 7E demonstrates that the tumor regression induced by dual blockade of CTLA-4/PD-1 was enhanced by respiratory hyperoxia.

DISCUSSION

This study demonstrates that the weakening of upstream tumor hypoxia by supplemental oxygenation decreases the intensity of the downstream A2AR-mediated immunosuppression in the TME. This, in turn, releases the restraints of the otherwise inhibited antitumor activities of T and NK cells and enables tumor regression and survival.

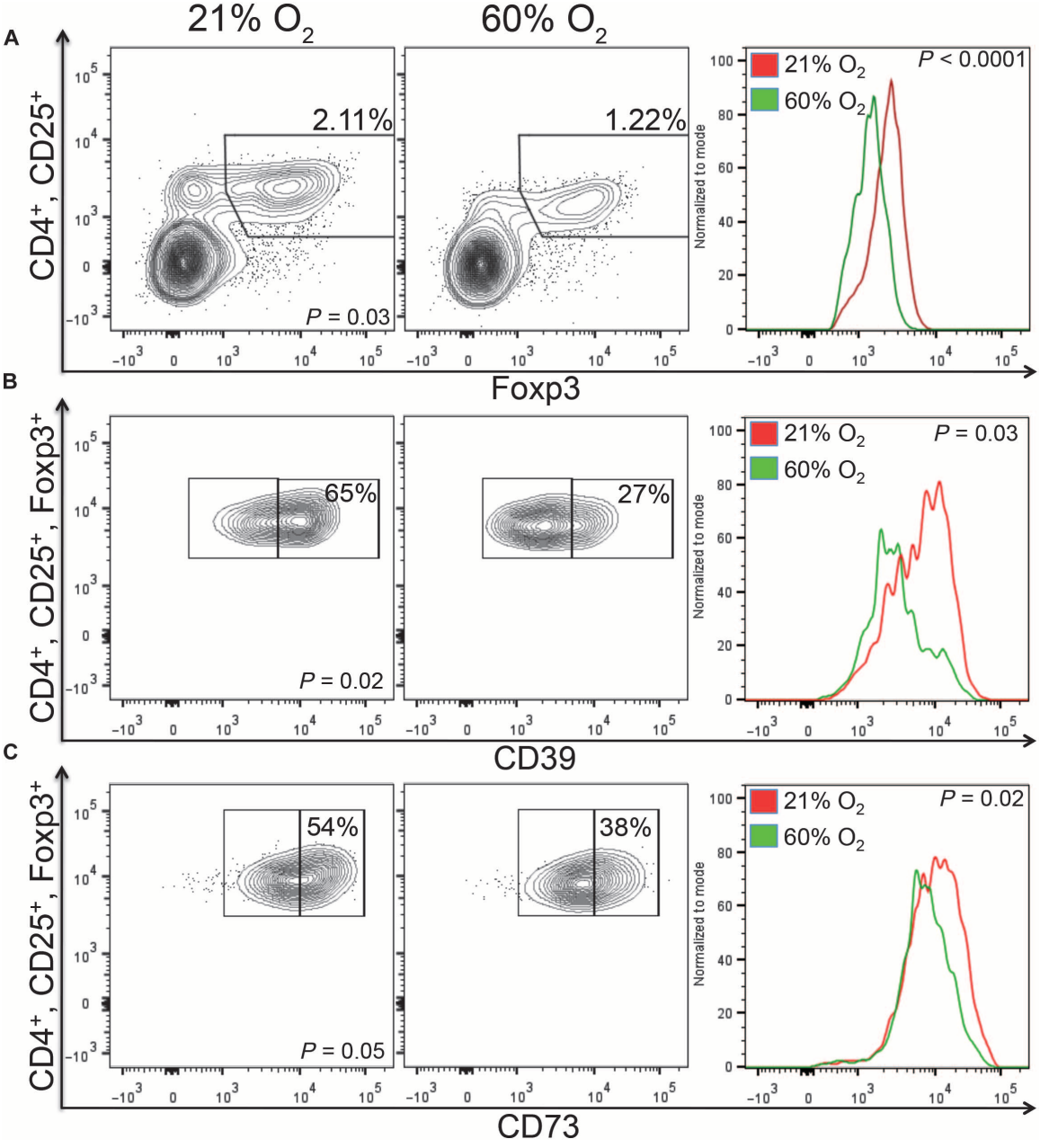

Fig. 5. Respiratory hyperoxia weakens immunosuppression by T_{regs} in the lung TME. (**A**) Left: Respiratory hyperoxia decreases the percentage of $CD4^+/CD25^+/Foxp3^+$ T_{regs} in the lung TME ($P = 0.03$; $n = 5$ mice per group). Mice bearing 11-day established MCA205 pulmonary tumors were placed in either 21 or 60% oxygen for 72 hours. Right: The expression of Foxp3 was also reduced by respiratory hyperoxia. The average MFI was 2227 and 1572 in mice breathing 21% versus 60% oxygen, respectively ($P = 5.82 \times 10^{-5}$; $n = 5$ mice per group). (**B** and **C**) Left: Respiratory hyperoxia reduces the expression of CD39 (B) and CD73 (C) on T_{regs} in the TME ($P = 0.02$ and $P = 0.05$; $n = 5$ mice per group). Right: The following are the average MFIs from 21 and 60% oxygen, respectively: CD39 (6329, 4226; $P = 0.03$) and CD73 (17054, 15761; $P = 0.02$).

These previously unappreciated and potentially medically valuable immunoenhancing antitumor effects of 60% oxygen were observed because of the assumption that oxygenation must be combined with the parallel activities of tumor-reactive T and NK cells. Indeed, these data demonstrate that the tumor-regressing effects of respiratory hyperoxia are dependent on the presence of T and NK cells. In accordance with earlier studies focused on the mechanisms of cytotoxicity, these data suggest that the improved tumor rejection could be accounted for by exocytosis of perforin-containing granules and by FAS-mediated cytotoxicity of antitumor T and NK cells unleashed by the weakening of hypoxia-adenosinergic immunosuppression (*39*). We recently demonstrated that respiratory hyperoxia induced the up-regulation of major histocompatibility complex class I on tumor cells, enhancing T cell–mediated cytotoxicity (*25*). This resulted in the increased recognition and destruction of tumor cells in vitro (*25*). Additionally, respiratory hyperoxia increased the production of proinflammatory cytokines and chemokines, including IFN-γ. This may contribute to starvation-induced apoptotic tumor cell death, potentially mediated by the increased levels of IFN-γ (*2*).

The use of respiratory hyperoxia offers a feasible direction in attempts to improve the immunotherapy of cancer by inhibiting not only the tumor-protecting hypoxia-CD39/CD73–mediated accumulation of immunosuppressive extracellular adenosine but also the hypoxia-driven formation of intracellular adenosine (*40*–*42*). This is another important potential source of extracellular adenosine (*40*–*42*). Hypoxia may increase the formation of intracellular adenosine by (i) decreasing intracellular levels of adenosine triphosphate, (ii) increasing intracellular AMP, (iii) inhibiting adenosine kinase, and (iv) increasing the expression of 5′-nucleotidase (*40*–*42*). Indeed, hypoxia/HIF-1α (hypoxia-inducible factor–1α)–driven inhibition of adenosine kinase leads to the accumulation of intracellular adenosine (*41*). This, in turn, may elevate levels of extracellular adenosine independent of CD39/CD73, further contributing to immune suppression (*16*–*19*, *21*, *42*).

It remains a possibility that suppression by tumor-associated macrophages (TAMs) or myeloid-derived suppressor cells (MDSCs) (*43*–*45*) might also be altered by the reversal of hypoxia. It has been well established that these cell types play an important role in tumor growth, metastasis, and suppression of the antitumor immune response. Moreover, it has recently been shown that hypoxia and HIF-1α drive the recruitment of MDSCs and TAMs to the TME, as well as M2-like polarization and activity (*43*–*45*).

Among the limitations of this study are the yet to be fully understood mechanisms of oxygenation-mediated de-inhibition of NK cells and

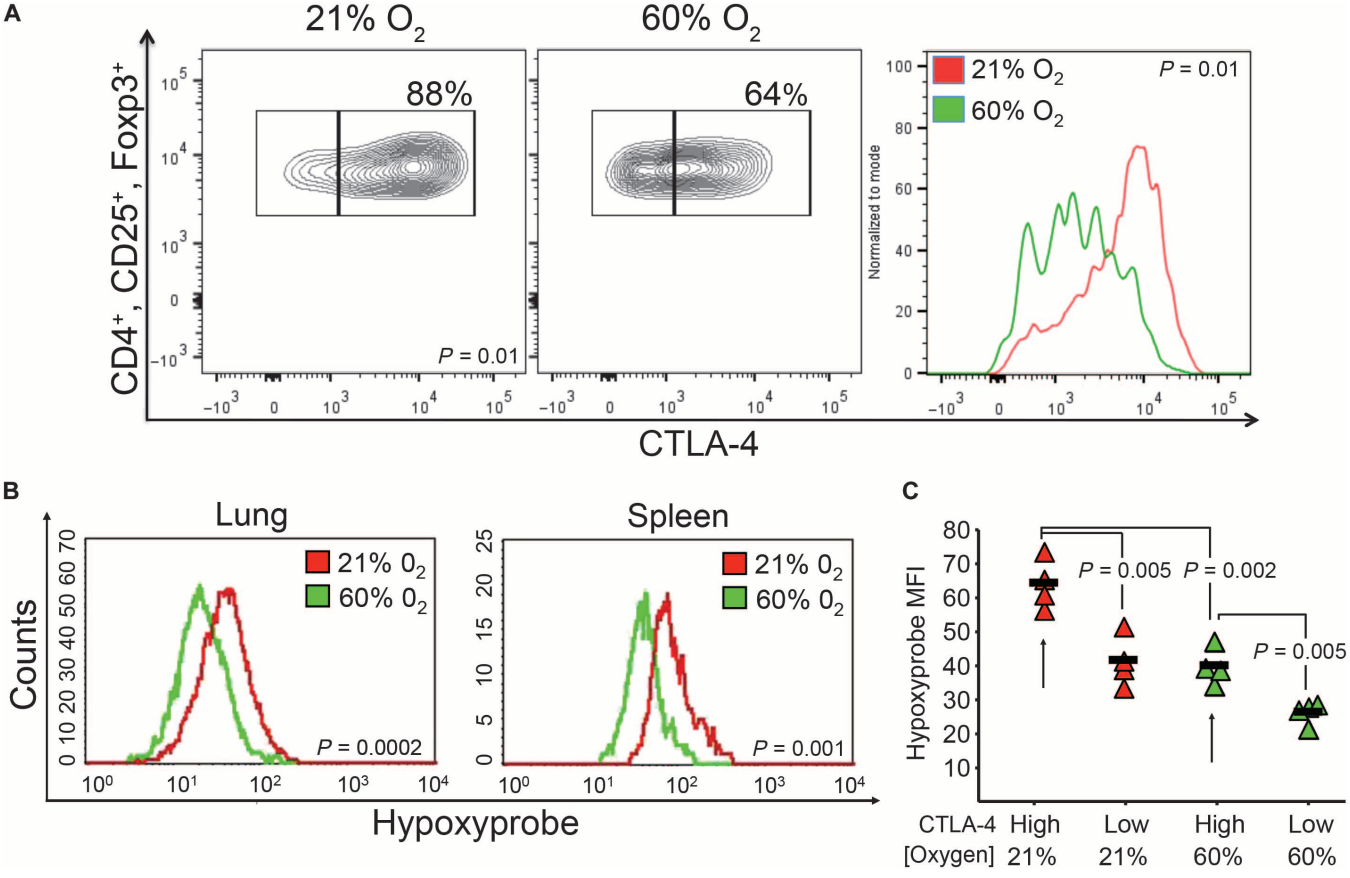

Fig. 6. Respiratory hyperoxia decreases exposure of T_{regs} to hypoxia and reduces expression of CTLA-4. (**A**) Respiratory hyperoxia reduces the expression of CTLA-4 by T_{regs}. The average MFI of CTLA-4 on T_{regs} was 4786 in mice breathing 21% O_2 and 2684 in mice breathing 60% O_2 ($P = 0.01$; $n = 5$ mice per group). (**B**) Respiratory hyperoxia reduces the exposure of T_{regs} to hypoxia in both the lung and the spleen of MCA205 tumor–bearing mice (lung: $P = 0.0002$, $n = 4$ mice per group; spleen: $P = 0.001$, $n = 3$ mice per group). (**C**) CTLA-4^{High} T_{regs} in the lung TME were also Hypoxyprobe^{High}, reflecting in vivo exposure to deeper levels of hypoxia. Respiratory hyperoxia decreased the numbers of CTLA-4^{High} T_{regs} compared to mice breathing 21% oxygen ($P = 0.002$; $n = 4$ mice per group).

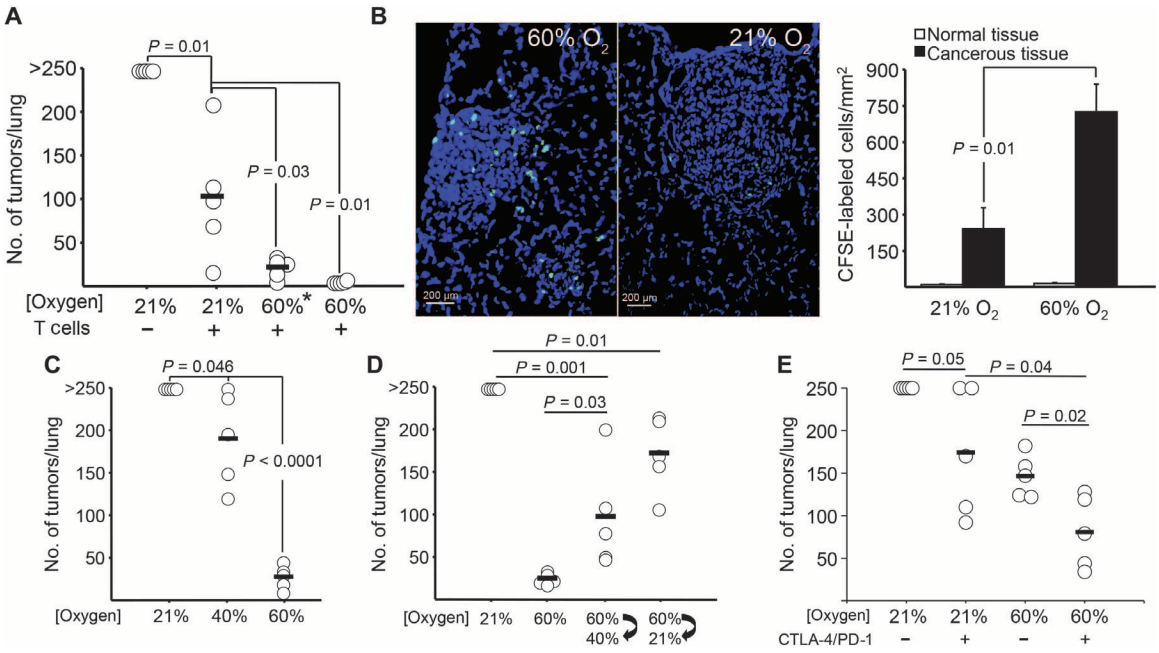

Fig. 7. Respiratory hyperoxia improves tumor regression in preclinical models of immunotherapies. (**A**) Adoptive immunotherapy in combination with respiratory hyperoxia enabled the complete regression of 11-day established MCA205 pulmonary tumors. Mice identified as 60%* were placed in the 60% oxygen units the same day as adoptive T cell immunotherapy, whereas mice identified as 60% were placed in oxygen units for the duration of the assay (21 days) [$n = 5$ mice per group, averages represented as horizontal bars; $P = 0.03$ (60%*) and $P = 0.01$ (60%)]. (**B**) Hyperoxia facilitates the infiltration of adoptively transferred T cells into 11-day established pulmonary tumors. Left: Fluorescent micrographs (scale bar, 200 μm) of CFSE-labeled adoptively transferred T cells (green) in mice breathing 60 or 21% oxygen 48 hours after adoptive transfer. Right: Enumeration of tumor-infiltrating transferred T cells. The average infiltration from ~100 tumors was 249 cells/mm^2 in control mice and 723 cells/mm^2 in mice breathing 60% oxygen ($n = 3$ mice per group; means ± SEM, $P = 0.01$). (**C**) Breathing as low as 40% oxygen results in pulmonary tumor regression [$n = 5$ mice per group, averages represented as horizontal bars; $P = 0.046$ (40% O_2) and $P = 3 \times 10^{-6}$ (60% O_2)]. (**D**) Alternating between breathing 60 and 40% oxygen or 60 and 21% oxygen every 12 hours enables tumor regression compared to mice continuously breathing 21% oxygen ($n = 5$ mice per group, averages represented as horizontal bars; $P = 0.001$ and $P = 0.01$, respectively). Breathing 60% oxygen continuously (24 hours/day) causes the strongest antitumor activity. (**E**) Respiratory hyperoxia improves the outcome of dual CTLA-4/PD-1 blockade in preclinical studies of lung tumor rejection. Mice were inoculated with MCA205 tumor cells and given mAbs for CTLA-4/PD-1 intraperitoneally on days 3, 6, and 9 (500 μg). Mice were treated with respiratory hyperoxia from days 3 to 21 or maintained at 21% O_2 until assay completion (day 21) ($n = 5$ mice per group, averages represented as horizontal bars; $P = 0.04$).

their potential role in orchestrating antitumor T cell responses. In addition, it is not yet clear whether the weakening of TME hypoxia in vivo affects the repertoire of activating versus inhibitory NK ligands.

An additional limitation exists in the requirement of 24-hour/day respiratory hyperoxia to accomplish the maximal outcome in these preclinical studies. However, the continuing advances in the design and use of high-oxygen masks may increase patient compliance with protocols of respiratory hyperoxia. A promising solution would be to decrease the required treatment time of respiratory hyperoxia by combining it with synthetic A2AR antagonists to further prevent immunosuppressive A2AR signaling by tumor-produced adenosine.

Although it is established that high levels of supplemental oxygen (>95% O_2) can cause oxygen toxicity as well as nonspecific inflammatory responses, the use of 60% oxygen is not associated with high-oxygen toxicity and is considered to be safe in long-term treatments (*22*). However, the delivery of 60% oxygen should be considered with an understanding that although long-term treatment has been proven to be safe, our previous reports attracted attention to the possibility that 60% oxygen may exacerbate ongoing acute inflammatory lung injury by inhibiting the hypoxia–HIF-1α–[adenosine]^{High}–A2AR pathway (*23*, *46*).

Therefore, it will be important to avoid using inhibitors of hypoxia–A2-adenosinergic immunosuppression, including respiratory hyperoxia, in cancer immunotherapy patients during simultaneous episodes of acute inflammation (*23*, *46*). Respiratory hyperoxia may not only enable stronger antitumor activities by de-inhibited tumor-reactive immune cells but also increase the inflammatory damage in normal tissues by de-inhibited myeloid cells or T cells activated by other antigens in patients with concomitant acute inflammation (*23*).

Because respiratory hyperoxia is widely used in clinical settings, it can be readily combined with existing immunotherapies for cancer and with already available and safe natural or synthetic antagonists of A2AR. We propose the clinical testing of respiratory hyperoxia either alone or in combination with the blockade of A2AR and inhibition of the CD39/CD73-mediated extracellular adenosine generation. It is expected that selective antagonists of A2AR will be most effective when combined with methods to reduce extracellular adenosine accumulation in the TME.

MATERIALS AND METHODS

Study design

The objective of this study was to test whether respiratory hyperoxia may prevent hypoxia-driven immunosuppression in the TME. The

tumor immunology assays in mice were expected to provide proof of principle for the potential therapeutic use of respiratory hyperoxia to overcome the inhibition of antitumor T and NK cells and improve tumor rejection. Sixty percent oxygen was selected because it is used in clinical protocols of respiratory hyperoxia. Treatment of cancer patients with advanced lung metastasis was mimicked by treatment of mice with well-established lung tumors. The maximal antitumor capacity of respiratory hyperoxia was determined by commencing treatment soon after inoculation of tumors. The MCA205 tumor cell line was used because of the predictable time course and intensity of T cell response (*30*, *31*). The more aggressive B16 melanoma was used to represent poorly immunogenic tumors (*31*, *38*). Orthotopically grown, CD73-expressing 4T1 breast tumors were also used in this study to mimic human TNBCs.

We compared 40 to 60% oxygen to provide a clinical alternative that might increase patient compliance with protocols of respiratory hyperoxia. To extend the clinical applicability, respiratory hyperoxia was combined with two major types of immunotherapy by testing whether respiratory hyperoxia would improve the preclinical therapeutic efficacy of adoptive T cell immunotherapy and dual blockade of CTLA-4 and PD-1.

Sample sizes were predetermined on the basis of statistical considerations and on pilot experiments that indicated the number of mice per group needed to generate statistical significance. Two-sided testing was performed with a confidence level of 95% for statistical analyses. Littermate mice were given tumors and randomly assigned to experimental or control groups. Where possible, treatment groups were blinded until statistical analysis. All experiments were repeated at least twice to confirm findings, and representative experiments are shown. The experimental procedures were approved by the Institutional Animal Care and Use Committee at Northeastern University.

Animals

Female C57BL/6N (B6) or Balb/c mice, 8 to 12 weeks old, were purchased from Charles River Laboratories; B6/*Thy1.1* mice were purchased from The Jackson Laboratory; γc/*Rag-2*$^{-/-}$ mice were purchased from Taconic. These animals were housed in a specific pathogen–free environment according to the National Institutes of Health (NIH) guidelines. All animal experiments were conducted in accordance with Institutional Animal Care and Use Committee guidelines of Northeastern University.

Tumors

MCA205 fibrosarcoma is a 3-methylcholanthrene–induced tumor of B6 origin (*30*, *31*), and B16-F10.P1 is a poorly immunogenic subclone of the spontaneously arising B16/BL6 melanoma (*31*, *38*). For establishment of pulmonary tumors, B6 mice were injected intravenously with either 3×10^5 MCA205 or B16-F10.P1 tumor cells suspended in 200 μl of Hanks' balanced salt solution (HBSS). On day 21, MCA205 tumor–bearing lungs were counterstained with India ink, and tumors were enumerated. Lungs with more than 250 nodules were assigned >250 as the maximum number that can be counted reliably. For survival studies, B6 mice were injected intravenously with 0.75×10^5 MCA205 tumor cells suspended in 200 μl of HBSS. For establishment of solid tumors, B6 mice were injected intradermally with 1×10^5 MCA205 tumor cells suspended in 100 μl of HBSS. For studies of spontaneous metastasis of orthotopically grown breast tumors, 1×10^5 4T1 cells (*20*, *21*) were injected into the third mammary fat pad of Balb/c mice.

Hyperoxic breathing

Mice were placed in chambers with well-controlled gas composition to mimic protocols of supplemental oxygen delivery to humans (*23*). Self-contained oxygen generators (AirSep) were used to ensure that desired levels of oxygen were maintained inside each unit. Hypercapnic acidosis was avoided by replacing traditional mouse cage tops with aerated wire lids and by using Sodasorb (Grace & Co.) (*23*, *47*, *48*). Composition of inhaled gas inside units was confirmed by analyzing PCO_2 (partial pressure of CO_2) and PO_2 (partial pressure of O_2) values in an equilibrated atmosphere. CO_2 levels inside the chamber never exceeded 0.4%, whereas hypercapnia typically occurs at levels higher than 2%. Confirmation of the levels of CO_2 and O_2 in control and experimental groups treated with 21 or 60% oxygen was done in collaboration with R. Marsh (Northeastern University). Fractional concentrations of O_2 and CO_2 were monitored by pulling a sample from the chamber at a rate of 100 ml min^{-1} using a Sable Systems Model SS3 sample pump (Sable Systems). The gas sample was pulled in order through the following: (i) a column of Drierite to remove water vapor; (ii) a Sable Systems model CA-1 CO_2 analyzer to measure the fractional concentration of CO_2; and (iii) a Sable Systems model FC-10 O_2 analyzer to measure the fractional concentration of O_2. The O_2 analyzer was calibrated using dry, CO_2-free air that was assumed to be 20.95% oxygen, and the CO_2 analyzer was calibrated using a 5.0% calibration gas from Medical-Technical Gases. Analog signals from the gas analyzers were recorded on a Macintosh computer using a 16-bit A-D converter (ADInstruments model Sp16) and the application LabChart from ADInstruments.

Monoclonal antibodies

For depletion of subsets of T and NK cells, immune cells were depleted (by intraperitoneal injection of 500 μg of either GK1.5, YTS 169, PK-136, or isotype control, Bio X Cell) 2 days before tumor inoculation and 60% oxygen treatment, preventing attack by T or NK cells on tumor cells. To maintain immune cell depletion, mAbs (250 μg) were given intraperitoneally each week until assay completion (21 days). Rat immunoglobulin G (IgG) isotype controls were given to control mice at the same dose. For CTLA-4/PD-1 dual blockade, mAbs against CTLA-4 (9H10, Bio X Cell) and PD-1 (J43, Bio X Cell) were injected (500 μg) intraperitoneally into tumor-bearing mice on days 3, 6, and 9. Mice were treated with respiratory hyperoxia from days 3 to 21 or maintained at 21% O_2 until assay completion at day 21.

Evaluation of TME hypoxia

For hypoxic localization of T cells, mice with established lung or intradermally grown MCA205 tumors were injected with Hypoxyprobe-1 (80 mg/kg). After 1.5 hours of labeling, lungs were snap-frozen, 5-μm cryosections were prepared from 10 to 20 different cutting surfaces, and immunohistochemistry was performed. For hypoxic lymphocyte analysis, mice with 11-day established MCA205 lung tumors were placed in 21 or 60% oxygen for 48 hours, and the MFI of Hypoxyprobe-1 on T cells from the lung and spleen was analyzed by flow cytometry.

Immunohistochemistry and analysis of intratumoral T cells

The infiltration of endogenous CD4/CD8 T cells into lung tumor nodules was quantified by the Harvard Medical School Pathology Department at Brigham and Women's Hospital in analyses using Spectrum Plus and Aperio's ScanScope slide scanners. Mice with 11-day established MCA205 pulmonary tumors were treated with 60% oxygen or maintained at 21% oxygen. After 4 days, the infiltration of CD4 and CD8

T cells into ~50 different lesions per group was assessed in mice breathing 21 and 60% oxygen. Immunohistochemistry was performed using 4-μm-thick acetone-fixed, optimum cutting temperature compound (OCT)–embedded tissue sections. The slides were soaked in −20°C methanol–acetic acid for 2 min and then air-dried for 20 min at room temperature. Slides were pretreated with Peroxidase Block (Dako). Primary rabbit anti-CD8 or anti-CD4 antibody (BD Pharmingen) was applied at a concentration of 1:100 at room temperature for 1 hour. Rabbit anti-rat Ig antibody was applied at a concentration of 1:750 in Dako diluent for 1 hour. Slides were detected with anti-rabbit Envision+ kit (Dako). Immunoperoxidase staining was developed using a diaminobenzidine chromogen (Dako) and counterstained with hematoxylin. Cell number per unit area was calculated after tumors were annotated using Spectrum Plus and Aperio's ScanScope slide scanners by the Harvard Medical School Pathology Department at Brigham and Women's Hospital.

For analysis of the localization of T cells in the hypoxic versus normoxic TME, tumor-bearing lungs or intradermal tumors were imbedded with OCT compound and frozen in liquid nitrogen. Sections were cut at 5 μm and mounted on glass slides. Sections were fixed in 1:1 acetone/methanol solution and stained with fluorescent-labeled Hypoxyprobe-1, CD4, and CD8 antibodies at a concentration of 1:200 for 3 hours. The slides were washed and counterstained with 4′,6-diamidino-2-phenylindole (Molecular Probes). The numbers of T cells/mm^2 in >180 hypoxic versus normoxic areas in both lung and intradermal tumors were analyzed using ImageJ software (NIH, MacBiophotonics).

Analysis of lung TME and flow cytometry

For studies of TME-infiltrating lymphocytes, mice with 11-day established MCA205 pulmonary tumors were placed in either 21 or 60% oxygen for up to 4 days. Tumor-bearing lungs were homogenized and passed through a 70-μm strainer. Lymphocytes were recovered using 40% Percoll separation, incubated with mAbs (BD Pharmingen and eBioscience) in fluorescence-activated cell sorting (FACS) buffer (phosphate-buffered saline + 0.5% bovine serum albumin), and acquired on a FACSCalibur or FACSCalibur Cytek DxP 8. Using this method, >98% of the lymphocytes were determined to be live cells by propidium iodide staining. Lymphocytes were analyzed with a lymphoid gate using CellQuest (BD Biosciences) and FlowJo (Tree Star) softwares.

Reverse transcription polymerase chain reaction

Mice with 11-day established MCA205 pulmonary tumors were placed in either 21 or 60% oxygen for 72 hours. A custom 96-well RT-PCR array was developed (Sylvester Comprehensive Cancer Center), primer sets were synthesized (Sigma), and RT-PCR was performed using the RT^2 SYBR Green PCR Mastermix (SuperArray) on an Applied Biosciences 7300 PCR platform as described previously (*35*). Housekeeping genes *Hrpt-1* and β-*actin* were used as controls. See table S2 for primer sequences.

Western blot

Mice with 11-day established lung tumors were placed in either 60 or 21% oxygen for 72 hours. Lungs were snap-frozen in liquid nitrogen and then homogenized in lysis buffer. After fractionation with SDS–polyacrylamide gel electrophoresis followed by semidry transfer, TGF-β in samples was detected with rabbit anti-mouse TGF-β polyclonal antibody conjugated to horseradish peroxidase (1:500, Santa Cruz). Levels of β-actin were detected using anti-mouse β-actin mAb (1:5000, Sigma-Aldrich).

Preparation of TDLN T cells for adoptive immunotherapy

B6 mice were inoculated subcutaneously with 1 × 10^6 MCA205 tumor cells in both flanks. Twelve days later, inguinal TDLNs were harvested, and single-cell suspensions were prepared and culture-activated as described previously (*30*, *31*, *49*). Four days later, TDLN cells (Fig. 7) were resuspended in HBSS for adoptive immunotherapy (*30*, *31*, *49*). Therapeutic efficacy of transferred T effector cells was assessed in the treatment of 11-day established MCA205 pulmonary tumors by intravenous injection of 5 × 10^6 culture-activated T cells to each mouse. Tumor-bearing mice were pretreated intravenously with cyclophosphamide (100 mg/kg) 1 day before infusion of T cells. Cyclophosphamide treatment is routinely used to improve the therapeutic efficacy of adoptively transferred T cells and was also administered to untreated tumor-bearing control mice (*38*, *49*).

Assessment of in vivo trafficking and cytokine production of tumor-reactive T cells

For fluorochrome labeling, cells were resuspended at 1 × 10^7/ml in HBSS containing 5 μM CFSE (Molecular Probes) as previously described (*31*). Forty-eight hours after transfer of 5 × 10^6 CFSE-labeled culture-activated TDLN T cells into tumor-bearing mice, lung samples were harvested and fixed in 4% formalin for 24 hours and then placed in 30% sucrose. Tissues were snap-frozen, and 5-μm cryosections were prepared from 10 to 20 different cutting surfaces. The number of CFSE-labeled cells in ~100 tumors from three mice per group was averaged and presented as the number of cells per mm^2 tumor tissue. Significance was evaluated by a Mann-Whitney test ($P = 0.01$). For cytokine analysis, TDLN T cells (5 × 10^6) derived from donor B6/Thy1.1$^+$ congenic mice were labeled with CFSE and injected into B6/Thy1.2$^+$ tumor-bearing recipients. Four days after transfer, Thy1.1$^+$ and Thy1.2$^+$ T cells were isolated from tumor-bearing lungs (~150 to 200 nodules), incubated with anti-CD3 (0.1 μM) for 4 hours, and analyzed by flow cytometry for the production of IFN-γ.

Statistics

The significance of differences in the numbers of pulmonary tumors between groups was measured by the Student's *t* test (two-sided), and tumor-bearing lung weights were analyzed by the Wilcoxon rank sum test. Survival studies of MCA205 tumor–bearing mice were analyzed using the log-rank test. Differences in hypoxic staining, cell numbers, RNA levels, tumor size, and flow cytometry data were analyzed by the Student's *t* test. The infiltration of transferred T cells was analyzed by the Mann-Whitney test. *P* values are listed within the figures and figure legends.

SUPPLEMENTARY MATERIALS

www.sciencetranslationalmedicine.org/cgi/content/full/7/277/277ra30/DC1

Materials and Methods

Fig. S1. The tumor-regressing effects of respiratory hyperoxia are lost in cγ/*Rag-2*$^{-/-}$ mice.

Fig. S2. ROS scavenger does not prevent the antitumor effects of respiratory hyperoxia.

Fig. S3. Respiratory hyperoxia reverses hypoxia-adenosinergic inhibition of NK cells.

Fig. S4. Respiratory hyperoxia does not further improve the activity of tumor-reactive A2AR$^{-/-}$ T cells.

Fig. S5. CD8 and CD4 T cells avoid hypoxic TME.

Fig. S6. T_{regs} with higher expression of CTLA-4 are more hypoxic.

Fig. S7. CD8 T cells from TDLN are enriched after culture activation for adoptive transfer.
Fig. S8. Breathing 60% oxygen increased IFN-γ production by CD8 T cells in the lung TME.
Table S1. Immunostimulating cytokines/chemokines increased by respiratory hyperoxia.
Table S2. Full list of primer sets in RT-PCR arrays.

REFERENCES AND NOTES

1. A. Ohta, M. Sitkovsky, Role of G-protein-coupled adenosine receptors in downregulation of inflammation and protection from tissue damage. *Nature* **414**, 916–920 (2001).
2. A. Ohta, E. Gorelik, S. J. Prasad, F. Ronchese, D. Lukashev, M. K. K. Wong, X. Huang, S. Caldwell, K. Liu, P. Smith, J.-F. Chen, E. K. Jackson, S. Apasov, S. Abrams, M. Sitkovsky, A2A adenosine receptor protects tumors from antitumor T cells. *Proc. Natl. Acad. Sci. U.S.A.* **103**, 13132–13137 (2006).
3. H. K. Eltzschig, M. V. Sitkovsky, S. C. Robson, Purinergic signaling during inflammation. *N. Engl. J. Med.* **367**, 2322–2333 (2012).
4. T. Raskovalova, X. Huang, M. Sitkovsky, L. C. Zacharia, E. K. Jackson, E. Gorelik, G_s protein-coupled adenosine receptor signaling and lytic function of activated NK cells. *J. Immunol.* **175**, 4383–4391 (2005).
5. M. V. Sitkovsky, T regulatory cells: Hypoxia-adenosinergic suppression and re-direction of the immune response. *Trends Immunol.* **30**, 102–108 (2009).
6. M. V. Sitkovsky, S. Hatfield, R. Abbott, B. Belikoff, D. Lukashev, A. Ohta, Hostile, hypoxia–A2-adenosinergic tumor biology as the next barrier to overcome for tumor immunologists. *Cancer Immunol. Res.* **2**, 598–605 (2014).
7. S. A. Rosenberg, N. P. Restifo, J. C. Yang, R. A. Morgan, M. E. Dudley, Adoptive cell transfer: A clinical path to effective cancer immunotherapy. *Nat. Rev. Cancer* **8**, 299–308 (2008).
8. P. Sharma, K. Wagner, J. D. Wolchok, J. P. Allison, Novel cancer immunotherapy agents with survival benefit: Recent successes and next steps. *Nat. Rev. Cancer* **11**, 805–812 (2011).
9. J. Naidoo, D. B. Page, J. D. Wolchok, Immune modulation for cancer therapy. *Br. J. Cancer* **111**, 2214–2219 (2014).
10. I. Mellman, G. Coukos, G. Dranoff, Cancer immunotherapy comes of age. *Nature* **480**, 480–489 (2011).
11. F. S. Hodi, S. J. O'Day, D. F. McDermott, R. W. Weber, J. A. Sosman, J. B. Haanen, R. Gonzalez, C. Robert, D. Schadendorf, J. C. Hassel, W. Akerley, A. J. van den Eertwegh, J. Lutzky, P. Lorigan, J. M. Vaubel, G. P. Linette, D. Hogg, C. H. Ottensmeier, C. Lebbé, C. Peschel, I. Quirt, J. I. Clark, J. D. Wolchok, J. S. Weber, J. Tian, M. J. Yellin, G. M. Nichol, A. Hoos, W. J. Urba, Improved survival with ipilimumab in patients with metastatic melanoma. *N. Engl. J. Med.* **363**, 711–723 (2010).
12. D. M. Pardoll, The blockade of immune checkpoints in cancer immunotherapy. *Nat. Rev. Cancer* **12**, 252–264 (2012).
13. A. Young, D. Mittal, J. Stagg, M. J. Smyth, Targeting cancer-derived adenosine: New therapeutic approaches. *Cancer Discov.* **4**, 879–888 (2014).
14. C. M. Koebel, W. Vermi, J. B. Swann, N. Zerafa, S. J. Rodig, L. J. Old, M. J. Smyth, R. D. Schreiber, Adaptive immunity maintains occult cancer in an equilibrium state. *Nature* **450**, 903–907 (2007).
15. A. T. Waickman, A. Alme, L. Senaldi, P. E. Zarek, M. Horton, J. D. Powell, Enhancement of tumor immunotherapy by deletion of the A_{2A} adenosine receptor. *Cancer Immunol. Immunother.* **61**, 917–926 (2012).
16. B. M. Künzli, M. I. Bernlochner, S. Rath, S. Käser, E. Csizmadia, K. Enjyoji, P. Cowan, A. d'Apice, K. Dwyer, R. Rosenberg, A. Perren, H. Friess, C. A. Maurer, S. C. Robson, Impact of CD39 and purinergic signalling on the growth and metastasis of colorectal cancer. *Purinergic Signal.* **7**, 231–241 (2011).
17. J. Stagg, U. Divisekera, N. McLaughlin, J. Sharkey, S. Pommey, D. Denoyer, K. M. Dwyer, and M. J. Smyth, Anti-CD73 antibody therapy inhibits breast tumor growth and metastasis. *Proc. Natl. Acad. Sci. U.S.A.* **107**, 1547–1552 (2010).
18. J. Stagg, U. Divisekera, H. Duret, T. Sparwasser, M. W. L. Teng, P. K. Darcy, M. J. Smyth, CD73-deficient mice have increased antitumor immunity and are resistant to experimental metastasis. *Cancer Res.* **71**, 2892–2900 (2011).
19. D. Jin, J. Fan, L. Wang, L. F. Thompson, A. Liu, B. J. Daniel, T. Shin, T. J. Curiel, B. Zhang, CD73 on tumor cells impairs antitumor T-cell responses: A novel mechanism of tumor-induced immune suppression. *Cancer Res.* **70**, 2245–2255 (2010).
20. P. A. Beavis, U. Divisekera, C. Paget, M. T. Chow, L. B. John, C. Devaud, K. Dwyer, J. Stagge, M. J. Smyth, P. K. Darcy, Blockade of A_{2A} receptors potently suppresses the metastasis of $CD73^+$ tumors. *Proc. Natl. Acad. Sci. U.S.A.* **110**, 14711–14716 (2013).
21. S. Loi, S. Pommey, B. Haibe-Kains, P. A. Beavis, P. K. Darcy, M. J. Smyth, J. Stagg, CD73 promotes anthracycline resistance and poor prognosis in triple negative breast cancer. *Proc. Natl. Acad. Sci. U.S.A.* **110**, 11091–11096 (2013).
22. R. H. Kallet, M. A. Matthay, Hyperoxic acute lung injury. *Respir. Care* **58**, 123–141 (2013).
23. M. Thiel, A. Chouker, A. Ohta, E. Jackson, C. Caldwell, P. Smith, D. Lukashev, I. Bittmann, M. V. Sitkovsky, Oxygenation inhibits the physiological tissue-protecting mechanism and thereby exacerbates acute inflammatory lung injury. *PLOS Biol.* **3**, e174 (2005).
24. P. Vaupel, Tumor oxygenation: An appraisal of past and present concepts and a look into the future: Arisztid G. B. Kovách Lecture. *Adv. Exp. Med. Biol.* **789**, 229–236 (2013).
25. S. M. Hatfield, J. Kjaergaard, D. Lukashev, B. Belikoff, T. H. Schreiber, S. Sethumadhavan, R. Abbott, P. Philbrook, M. Thayer, D. Shujia, S. Rodig, J. L. Kutok, J. Ren, A. Ohta, E. R. Podack, B. Karger, E. K. Jackson, M. Sitkovsky, Systemic oxygenation weakens the hypoxia and hypoxia inducible factor 1α-dependent and extracellular adenosine-mediated tumor protection. *J. Mol. Med.* **92**, 1283–1292 (2014).
26. M. W. Dewhirst, Y. Cao, B. Moeller, Cycling hypoxia and free radicals regulate angiogenesis and radiotherapy response. *Nat. Rev. Cancer* **8**, 425–437 (2008).
27. J. Wang, J. Yi, Cancer cell killing via ROS: To increase or decrease, that is the question. *Cancer Biol. Ther.* **7**, 1875–1884 (2008).
28. J. H. Min, C. N. Codipilly, S. Nasim, E. J. Miller, M. N. Ahmed, Synergistic protection against hyperoxia-induced lung injury by neutrophils blockade and EC-SOD overexpression. *Respir. Res.* **13**, 58 (2012).
29. E. Kratzer, Y. Tian, N. Sarich, T. Wu, A. Meliton, A. Leff, A. A. Birukova, Oxidative stress contributes to lung injury and barrier dysfunction via microtubule destabilization. *Am. J. Respir. Cell Mol. Biol.* **47**, 688–697 (2012).
30. J. Kjaergaard, S. Shu, Tumor infiltration by adoptively transferred T cells is independent of immunologic specificity but requires down-regulation of L-selectin expression. *J. Immunol.* **163**, 751–759 (1999).
31. J. Kjaergaard, L. Peng, P. A. Cohen, S. Shu, Therapeutic efficacy of adoptive immunotherapy is predicated on in vivo antigen-specific proliferation of donor T cells. *Clin. Immunol.* **108**, 8–20 (2003).
32. M. Champsaur, L. L. Lanier, Effect of NKG2D ligand expression on host immune responses. *Immunol. Rev.* **235**, 267–285 (2010).
33. D. H. Raulet, S. Gasser, B. G. Gowen, W. Deng, H. Jung, Regulation of ligands for the NKG2D activating receptor. *Annu. Rev. Immunol.* **31**, 413–441 (2013).
34. S. A. Quezada, K. S. Peggs, T. R. Simpson, Y. Shen, D. R. Littman, J. P. Allison, Limited tumor infiltration by activated T effector cells restricts the therapeutic activity of regulatory T cell depletion against established melanoma. *J. Exp. Med.* **205**, 2125–2138 (2008).
35. T. H. Schreiber, V. V. Deyev, J. D. Rosenblatt, E. R. Podack, Tumor-induced suppression of CTL expansion and subjugation by gp96-Ig vaccination. *Cancer Res.* **69**, 2026–2033 (2009).
36. M. V. Sitkovsky, J. Kjaergaard, D. Lukashev, A. Ohta, Hypoxia-adenosinergic immunosuppression: Tumor protection by T regulatory cells and cancerous tissue hypoxia. *Clin. Cancer Res.* **14**, 5947–5952 (2008).
37. K. Wing, Y. Onishi, P. Prieto-Martin, T. Yamaguchi, M. Miyara, Z. Fehervari, T. Nomura, S. Sakaguchi, CTLA-4 control over $Foxp3^+$ regulatory T cell function. *Science* **322**, 271–275 (2008).
38. J. Kjaergaard, L. Peng, P. A. Cohen, J. A. Drazba, A. D. Weinberg, S. Shu, Augmentation versus inhibition: Effects of conjunctional OX-40 receptor monoclonal antibody and IL-2 treatment on adoptive immunotherapy of advanced tumor. *J. Immunol.* **167**, 6669–6677 (2001).
39. M. Koshiba, H. Kojima, S. Huang, S. Apasov, M. V. Sitkovsky, Memory of extracellular adenosine A_{2A} purinergic receptor-mediated signaling in murine T cells. *J. Biol. Chem.* **272**, 25881–25889 (1997).
40. S. Kobayashi, H. Zimmermann, D. E. Millhorn, Chronic hypoxia enhances adenosine release in rat PC12 cells by altering adenosine metabolism and membrane transport. *J. Neurochem.* **74**, 621–632 (2000).
41. U. K. Decking, G. Schlieper, K. Kroll, J. Schrader, Hypoxia-induced inhibition of adenosine-kinase potentiates cardiac adenosine release. *Circ. Res.* **81**, 154–164 (1997).
42. K. Synnestvedt, G. T. Furuta, K. M. Comerford, N. Louis, J. Karhausen, H. K. Eltzschig, K. R. Hansen, L. F. Thompson, S. P. Colgan, Ecto-5′-nucleotidase (CD73) regulation by hypoxia-inducible factor-1 mediates permeability changes in intestinal epithelia. *J. Clin. Invest.* **110**, 993–1002 (2002).
43. C. A. Corzo, T. Condamine, L. Lu, M. J. Cotter, J. I. Youn, P. Cheng, H. I. Cho, E. Celis, D. G. Quiceno, T. Padhya, T. V. McCaffrey, J. C. McCaffrey, D. I. Gabrilovich, HIF-1α regulates function and differentiation of myeloid-derived suppressor cells in the tumor microenvironment. *J. Exp. Med.* **207**, 2439–2453 (2010).
44. O. R. Colegio, N.-Q. Chu, A. L. Szabo, T. Chu, A. Marie Rhebergen, V. Jairam, N. Cyrus, C. E. Brokowski, S. C. Eisenbarth, G. M. Phillips, G. W. Cline, A. J. Phillips, R. Medzhitov, Functional polarization of tumour-associated macrophages by tumour-derived lactic acid. *Nature* **513**, 559–563 (2014).
45. P. Chaturvedi, D. M. Gilkes, N. Takano, G. L. Semenza, Hypoxia-inducible factor-dependent signaling between triple-negative breast cancer cells and mesenchymal stem cells promotes macrophage recruitment. *Proc. Natl. Acad. Sci. U.S.A.* **111**, E2120–E2129 (2014).
46. A. Ohta, M. Sitkovsky, Caveats in promising therapeutic targeting of the anti-inflammatory A2 adenosine receptors: The notes of caution. *Nat. Rev. Drug Discov.* **5** (2006).
47. H. Ooi, E. Cadogan, M. Sweeney, K. Howell, R. G. O'Regan, P. McLoughlin, Chronic hypercapnia inhibits hypoxic pulmonary vascular remodeling. *Am. J. Physiol. Heart Circ. Physiol.* **278**, H331–H338 (2000).

48. H. R. De Smet, A. D. Bersten, H. A. Barr, I. R. Doyle, Hypercapnic acidosis modulates inflammation, lung mechanics, and edema in the isolated perfused lung. *J. Crit. Care* **22**, 305–313 (2007).
49. J. Kjaergaard, J. Tanaka, J. A. Kim, K. Rothchild, A. Weinberg, S. Shu, Therapeutic efficacy of OX-40 receptor antibody depends on tumor immunogenicity and anatomic site of tumor growth. *Cancer Res.* **60**, 5514–5521 (2000).

Acknowledgments: We thank J. Stagg at the University of Montreal for providing the 4T1 tumor cell line and sharing his expertise. We thank S. Ohman for assistance in all steps leading to the preparation of the manuscript. We also thank R. Marsh, professor of biology at Northeastern University, for assistance with monitoring and controlling gas levels in hyperoxic units. **Funding:** This work was supported by funding from Northeastern University and NIH grants to M.V.S. (R01 CA 112561, R01 CA 111985, R21 AT 002788, U19 AI 091693, Dana-Farber Cancer Institute, and Harvard Medical School–Northeastern University Joint Program in Cancer Drug Development) as well as by National Cancer Institute grant 5PO1CA109094-03 and National Institute of Allergy and Infectious Diseases 1P01 grant AI096396-01 3 to E.R.P.; HL109002, DK091190, DK068575, DK079307, and CA168628 to E. K. J.; and a Bankhead-Coley Postdoctoral Fellowship to T.H.S. **Author contributions:** S.M.H., J.K., A.O., and M.V.S. performed and/or analyzed cancer immunology assays. S.R. and J.L.K. performed, enumerated, and interpreted immunohistochemistry assays. J.K. established and supervised lung tumor models. E.R.P. and T.H.S. designed and performed assays with custom-made RNA arrays to scan lung TME. D.L., B.B., R.A., S.S., P.P., K.K., R.C., and M.T. performed or assisted in tumor immunology, immunohistochemistry, and flow cytometry assays. E.K.J. and B.K. analyzed and interpreted changes in the TME. M.V.S. designed the overall approach, directed all stages of research, and wrote the manuscript with S.M.H. **Competing interests:** U.S. government, NIH holds an issued patent "Methods for using extracellular adenosine inhibitors and adenosine receptor inhibitors to enhance immune response and inflammation," US 8,716,301, which is related to the work described in this paper, with A.O. and M.V.S. named as inventors. M.V.S. is a founder of RedoxTherapies, a company that is charged with the translation of this approach into the clinic and has licensed this patent. E.R.P. has a provisional patent for "Anti-immune suppression tumor therapy" and is the scientific cofounder, paid consultant, and equity owner of Heat Biologics Inc., and T.H.S. is an employee at Heat Biologics Inc. J.L.K. is an employee and shareholder at Infinity Pharmaceuticals Inc. E.K.J. holds equity in Adenopaint, which is unrelated to the current study. **Data and materials availability:** Correspondence and requests for materials should be addressed to M.V.S. (m.sitkovsky@neu.edu).

Submitted 23 October 2014
Accepted 28 January 2015
Published 4 March 2015
10.1126/scitranslmed.aaa1260

Citation: S. M. Hatfield, J. Kjaergaard, D. Lukashev, T. H. Schreiber, B. Belikoff, R. Abbott, S. Sethumadhavan, P. Philbrook, K. Ko, R. Cannici, M. Thayer, S. Rodig, J. L. Kutok, E. K. Jackson, B. Karger, E. R. Podack, A. Ohta, M. V. Sitkovsky, Immunological mechanisms of the antitumor effects of supplemental oxygenation. *Sci. Transl. Med.* **7**, 277ra30 (2015).

Science Translational Medicine
AAAS

Immunological mechanisms of the antitumor effects of supplemental oxygenation

Stephen M. Hatfield *et al.*

Sci Transl Med **7**, 277ra30 (2015);
DOI: 10.1126/scitranslmed.aaa1260

Editor's Summary

Paving the way for intratumoral T cells

Tumors often express unusual antigens and are surrounded by immune cells. Unfortunately, this immune surveillance is imperfect and does not always prevent the tumors from growing. In addition, tumors are often hypoxic, because their rapid growth outstrips that of their blood and oxygen supply. Now, Hatfield *et al.* have linked these two phenomena by demonstrating that T cells avoid going into the hypoxic areas of tumors. The authors have also shown a way to overcome this problem in mice with lung tumors by having the animals breathe supplementary oxygen. Having a higher concentration of oxygen throughout the body improved the oxygenation inside the tumors, allowing immune cells to enter the tumors and attack them, extending the animals' survival.

Science Translational Medicine (print ISSN 1946-6234; online ISSN 1946-6242) is published weekly, except the last week in December, by the American Association for the Advancement of Science, 1200 New York Avenue NW, Washington, DC 20005.